Investigation of Structural Features of As_2S_3-Se Multilayer Nanostructure by Raman Spectroscopy

V. Abaskin[a], *E. Achimova[a], A. Meshalkin[a], A. Prisacar[a], G. Triduh[a], M. Vlcek[b], L. Loghina[b], I. Voynarovich[b]

[a]Institute of Applied Physics, Academy of Sciences of Moldova,
*Academiei str. 5, MD-2028, Chisinau, Moldova, *e-mail: achimova@phys.asm.md*
[b]Department of General and Inorganic Chemistry,
Faculty of Chemical Technology, University of Pardubice, 53210 Pardubice, Czech Republic

The focus of this research is on the investigation of structural changes in the As_2S_3-Se multilayer nanostructure and on the examination of a relative contribution of As_2S_3 and Se layers to nanostructuring by measuring the Raman spectra. The formation of the As_2S_3-Se nanostructure by an alternate As_2S_3 and Se layers deposition was applied. The diffraction efficiency dependence on the exposure of a CW DPSS laser were monitored in a transmission mode of the1st order diffracted beam intensity and measured in real-time at the normal incidence of the laser diode beam (λ = 650 nm). From the comparison of these dependences for a set of samples we have chosen the multilayer nanostructure As_2S_3-Se with optimal recording properties meaning maximum both the value and the rate of diffraction efficiency. Our results are found to be of practical interest as they allow a significant improvement of the diffraction efficiency of the directly recorded relief gratings.

Keywords: chalcogenide glasses, nanostructures, Raman spectroscopy, surface grating.

УДК 535.4; 538.958; 538.975

INTRODUCTION

In the last two decades, much research work has been focused on the formation of a nanostructure suitable for micro- nano-electronics and photonics applications. Glasses are promising materials for these areas for two reasons. First, the control of nanostructures could give the information about their glassy structure. Unlike crystalline materials, in which we can prepare atomically controlled surfaces, the amorphous structure is disordered at the atomic level. Second, the glass nanostructure may yield a wider variety than the crystalline one because the bonding constraints of crystals do not exist in glasses [1].

A growing interest in the research of chalcogenide glasses (ChGs) can be currently witnessed, which, to a large extent, is caused by newly opened fields of applications for these materials. Among glasses, chalcogenides possess unique characteristics different from those in oxide and halide glasses, i.e., molecular (low-dimensional) structures and semiconductor properties. ChGs appear to be attractive materials for the investigation of nano-structural properties mainly due to photo-induced changes in their structure and properties. Their unique photo-structural properties allow processing of optical elements upon irradiation with sub-bandgap light through direct writing or holographic methods [2, 3].

The interplay between a micro-structure and desirable properties of devices may be illustrated in micro nanostructures suitable for usage in high performance diffraction optical elements (DOE). These require a broad transmittance optical window and light switching capabilities which must be compatible with the current system configurations, have both broadband linear and nonlinear indices of refraction, as well as low volume losses. ChGs are considered promising as they exhibit properties compatible with the mentioned above [4, 5].

The reason why ChGs exhibit many kinds of photo-induced phenomena can be ascribed to their unique electronic and atomic structures [6]. Electronically, ChGs are a kind of a semiconductor with the energy gap of 1–3 eV, and accordingly, it can be photo-excited by visible light. In addition, excited carriers are localized in disordered and defective glass structures, and the carriers undergo strong electron–lattice interaction. Structurally, ChGs have a moderate atomic connectivity, which is not as rigid as in oxide glasses nor as flexible as in inorganic polymers.

Raman spectroscopy permits to investigate the structure of amorphous materials through measurements of lattice vibration modes. In principle, each Raman scattering peak can be associated with a vibration of a specific structural unit [7, 8]. This intrinsic nano-probing makes Raman spectroscopy very sensitive to short and medium-range structures – including in glassy materials, and offers a “bottom-up” approach to nanostructured materials that comes as a good complement to methods like the transmission electron microscopy or X-ray diffraction. However, studies on nano-chalcogenides are still at an early

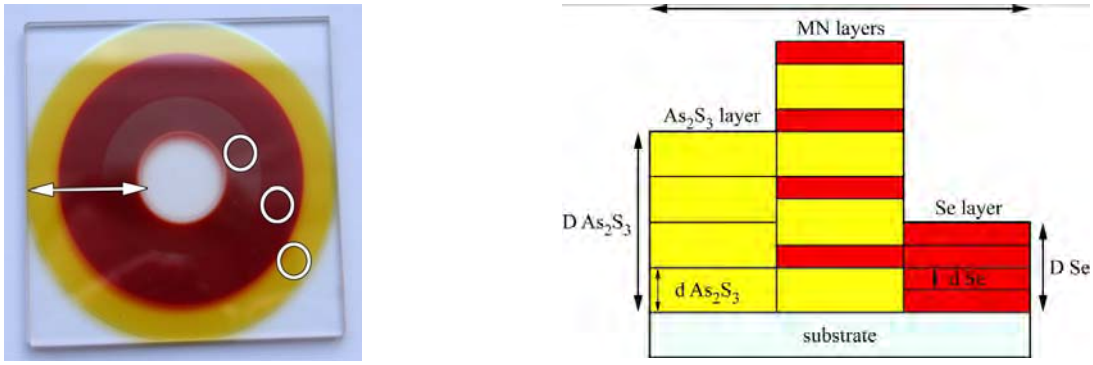

(a) (b)

Fig. 1. (a) Photograph of As_2S_3-Se MN sample on polished glass substrate (75x75 mm^2). White circles point of Raman spectra measurements locations. (b) Radial fragment of cross-section of 4 As_2S_3 and 4 Se nanolayers formed of nanostructure on substrate (as an example). Horizontal arrows (in Fig. 1a,b) point to the same part of the sample. The vertical arrow indicates total thickness $D_{As_2S_3}$ and D_{Se}, and thicknesses of one layer $d_{As_2S_3}$ and of one layer of d_{Se} respectively.

stage and need to be further extended to cover more ChGs, which is due to the primary remarkable results obtained in their nanostructure forms.

The aim of the present work is to extend the research of nanostructuring properties of the As_2S_3-Se multilayer nanostructure (MN) on the dimensions of constituent layers by measuring the Raman spectra. The purpose of this research is to investigate the structural changes in the As_2S_3-Se MN and, in particular, to examine the relative contribution of As_2S_3 and Se to nanostructuring. We have selected Se and As_2S_3 nanolayers as components for the As_2S_3-Se MN because of their known parameters and well-developed deposition technology. In addition, while chalcogens are good glass formers over a wide range of composition, a large majority of studies have focused on the stoichiometric chalcogenide As_2S_3 due to its good stability. Nevertheless, the formation of a nano-structure such as As_2S_3-Se is of much interest as the addition of Se nanolayer allows us to tune and change the optical transparency and to improve the recording properties.

METHODS OF STRUCTURE PREPARATION AND MEASUREMENTS

The bulk samples of As_2S_3 were synthesized by the melt-quenching technique from the components heated in evacuated quartz ampoules at T = 900°C for 30 hours.

ChG nanomultilayers were prepared by the computer controlled cyclic thermal vacuum successive deposition of two materials from two separated boats on a continuously rotated glass substrate at room temperature in one vacuum deposition cycle [9]. The technology allows thin films deposition with a thicknesses from 0.005 up to 3.0μm. The control of the total film thickness was carried out during the thermal evaporation by the interference thickness sensor at λ = 0.95 μm. The thickness of one layer was calculated dividing the total measured thickness on number of cycles. On the Figure 1 the photograph (Fig. 1a) and the cross-section (Fig. 1b) of the samples are shown. The overlapping part of the samples contains alternating nanolayers of Se and As_2S_3, i.e. two wide rings are overlapped in the central part of the substrate forming MNs. Outside and internal rings of the layers on the substrate contain pure compositions of As_2S_3 and Se, respectively. Pure compositions of As_2S_3 and Se layers here do not differ from those of the same kind of materials during deposition on a standard motionless substrate. Such control layers of As_2S_3 and Se we used to check the composition and calculate the ratio of the sub-layer thicknesses in one modulation period Λ (the total thickness of one As_2S_3 and one Se nanolayers). As a result, MN samples of the As_2S_3-Se type structures with the total thickness of 1.5–2.5 μm, the total number of nanolayers up to 100, the modulation periods of 15–50 nm range were obtained. The wide band-gap material As_2S_3 (E_g = 2.4 eV) was an optically transparent barrier and the active material Se had a narrower band-gap (E = 1.8 eV).

Such approach to the samples layers configuration is aimed at an effort to answer research questions, namely, size restriction of the constituent ChG layers of the samples. One deposition process gives a possibility to compare optical and Raman spectra of the constituents of As_2S_3 and Se layers separately, as well as to demonstrate the influence of thickness on the MN features.

Structural changes in differently exposed samples were studied by Raman spectroscopy. FT-Raman spectra were measured on a Bruker IFS 55 with a Bruker FRA 106 Raman module [10]. Near-IR Nd:YAG laser with a wavelength of 1064 nm (E = 1.17 eV) was used as excitation source. All measurements were performed at room temperature in back-scattering geometry.

An interferometric holographic recording was used to expose linear grating on the As_2S_3 film [11]. The period of the grating $d = \lambda/(2\sin\alpha)$, where λ is

the wavelength of a laser beam, α is the angle between the incidence laser beams. A CW DPSS single mode laser operated at 532 nm and a spot power density of 350 mW/cm^2 was used for recording. The holographic gratings with a period of d = 1000 lp/mm were recorded by two symmetrical angled laser beams with respect to the sample surface normal. The intensity ratio of the recording beams 1:1 was used in order to achieve the maximum visibility of interference fringes. Interfering beams with S–S polarization of recording laser beams was used for gratings formation. The experimental set up is sketched in Figure 2.

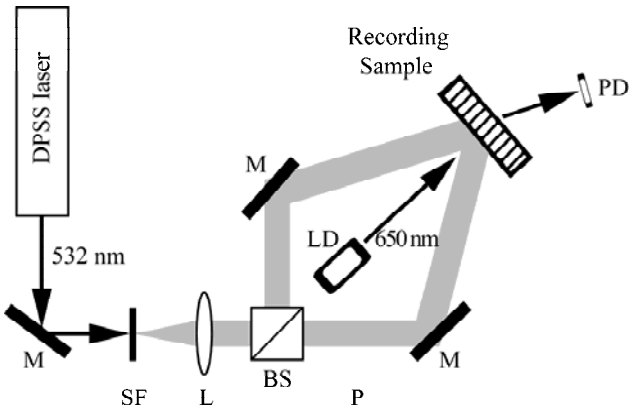

Fig. 2. Optical arrangement for holographic grating recording with real-time measurement of diffraction efficiency by photodetector. DPSS laser (532 nm, 50 mW), *M* – mirror; *SF* – spatial filter; *L* – collimating lens; *BS* – beam splitter; *LD* – laser diode (λ_{red} = 650 nm) for monitoring recording process; *PD* – photodetector.

RESULTS AND DISCUSSION

Inelastic scattering of light – or Raman scattering – from elementary excitations in a material yields structural and dynamic information on a molecular level. The Raman spectrum can be analyzed in terms of the molecular components or the functional groups thus providing a "fingerprint" of the molecule. A distinct advantage over other approaches that use the visible range of the spectrum is the ability to obtain the Raman spectrum of photosensitive compounds without interference from photoreactions caused by the probe beam. In ChGs the shifting of the excitation wavelength to 1064 nm (below the bandgap) allows one to obtain high quality Raman spectra and to correlate the underlying structure with optical properties.

The material of interest is the As_2S_3-Se MN with three modulation periods Λ pointed in Table 1. The examination of the Raman spectra of the As_2S_3-Se MN were carried out with the Raman spectra of separated As_2S_3 and Se non-overlapping layers.

The Raman spectra of three different As_2S_3 films corresponding to three modulation periods of the MNs are shown in Figure 3. Each Raman spectrum was fitted using a series of Gaussian peaks with a width appropriate for glasses. Table 2 provides a list of frequency as assignments of the known structural units in the As_2S_3 glass. These assignments were used to perform the peak-fitting analyses and to compare the relative contribution of each structural unit of As_2S_3. The Raman spectra reveal two main vibration bands located at 130–250 and 310–390 cm^{-1} (Fig. 3) which can be assigned to the vibration of the As-As containing units, such as As_4S_4, together with an additional band with maxima at 495 cm^{-1} [12]. These two bands indicate that S-S containing structural units such as -S-S-chains are present and connect individual S-S chains (495 cm^{-1}). Appearance of these structural units containing homopolar bonds in the structure of the evaporated As_2S_3 can be explained by the thermal dissociation reaction during evaporation, where a non-stoichiometric As_4S_4 unit contains a homopolar As-As bond. A weak band near 495 cm^{-1} indicates small numbers of S–S bonds. Due to fast condensation of vapours on the cold (at room temperature) substrate these structural units are frozen and thus responsible for the photosensitivity of these films.

Table 1. Multilayers nanostructure As_2S_3-Se thicknesses

	Test 1	Test 2	Test 3
Total thickness	2.5 μm	2.5 μm	1.5 μm
Number of nanolayers	50	100	100
Λ	50 nm	25 nm	15 nm
$d_{As_2S_3}$	30 nm	15 nm	8 nm
d_{Se}	20 nm	10 nm	7 nm
$D_{As_2S_3}$	1.5 μm	1.5 μm	0.8 μm
D_{Se}	1.0 μm	1.0 μm	0.7 μm

From Figure 3 it is clear that the peak positions coincide for three different As_2S_3 parts of the samples and correspond to results of other authors [14]. The intensities of all peaks are maxima for the maximal thickness of As_2S_3 $d_{As_2S_3}$ = 1.5 μm. In test 2 and test 3, the curves of Raman spectra are very close, but the plot of the sample with $d_{As_2S_3}$ = 1 μm (test 2) lies lower than that for the sample with $d_{As_2S_3}$ = 0.8 μm (test 3).

Figure 4 shows the Raman spectra of separated Se parts of films constituents in MN (tests 1, 2, and 3). For all MN the Raman spectra of pure Se films exhibit a strong band at 251.1 cm^{-1} and weaker bands at 110 cm^{-1} and 131.5 cm^{-1}, which are specific for Se_8 rings and fragments of Se_8 rings containing 5 and 6 Se atoms [15]. The shoulder near 233 cm^{-1} corresponds to Se chains and is clearly seen for the thinnest MN test 3. It is known that Se is a not stable material, but for the crystallization to occur, the size

Table 2. Vibrational mode frequencies

Peaks As_2S_3 from Figure 3	Peak assignments from [13]
135.4	As-As units
145.0	145.7, α(β)-As_4S_4
169.1	171.4, *p*-As_4S_4
189.4	182.6, α(β)-As_4S_4
223.1	221.0, α(β)-As_4S_4
233.7	238.4, *p*-As_4S_4
274.2	271.0, α(β)-As_4S_4
344.6	341.5, α(β)-As_4S_4
362.0	363.0, As-As units; α(β)-As_4S_4
495.0	495.0, S-S chains

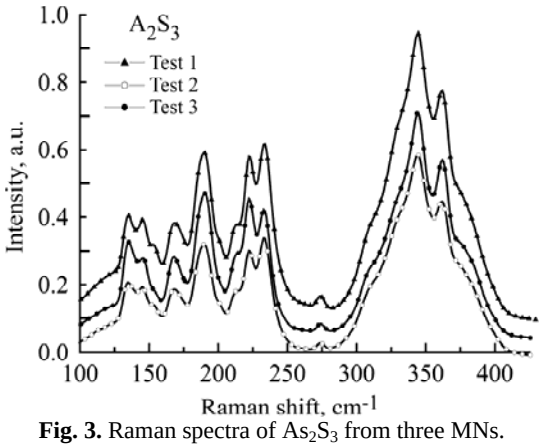

Fig. 3. Raman spectra of As_2S_3 from three MNs.

of Se films (clusters) should be greater than that of crystallites, which is probably 5–20 nm [16]. This requirement may be satisfied in the spatially-restricted test 1 and test 2, unlike test 3.

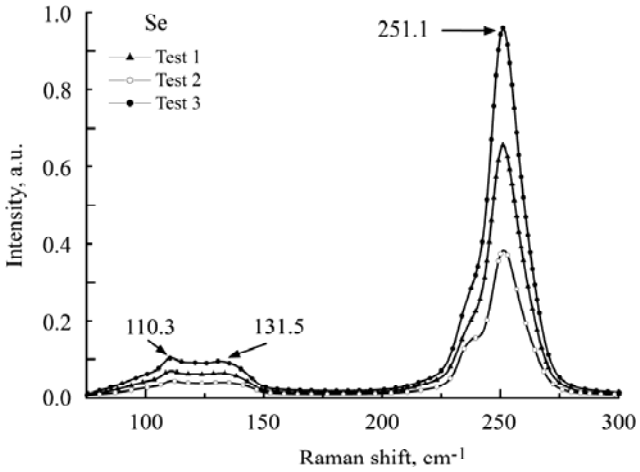

Fig. 4. Raman spectra of Se from three MNs.

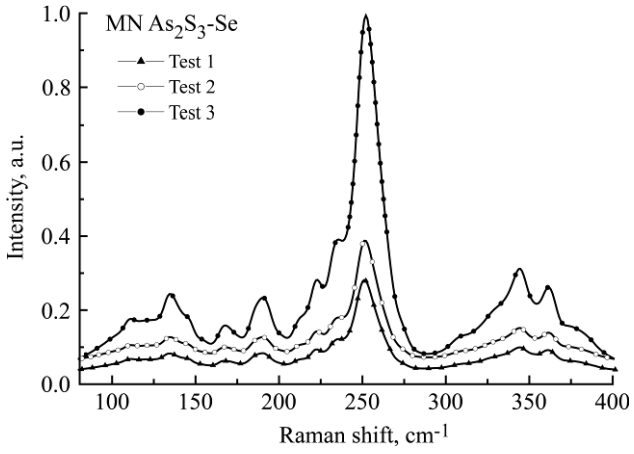

Fig. 5. Raman spectra of As_2S_3-Se MN with modulation period Λ = 50 nm (test 1), Λ = 25 nm (test 2), Λ = 15 nm (test 3).

Figure 5 gives the Raman spectra of the As_2S_3-Se MN for three types of the samples under test. As is seen, the Raman spectrum for the MN incorporates of Raman spectra of separated films constituent of the As_2S_3 and Se MNs. The position and shape of the peaks and their number says in favour of this. From the comparison of the Raman spectra for the MNs with different modulation periods, it is clear that the MN with Λ = 15 nm (test 3) has sharp and high-intensity peaks. These parameters of spectra (the peak sharpness and the arbitrary intensity) decrease with the modulation period increasing. This feature may be explained by the ordering of the MN structure. Lower the layer thickness leads to higher the degree of order of each constituent of the MN layers.

The Raman spectra of the As_2S_3-Se MN measured after illumination by 525 nm during 20 min are shown in Figure 6. The behaviour of Raman spectra after illumination is opposite the one before illumination in sense of the ordering of constituent layers. The peaks of the MN with larger modulation periods are of higher intensities and sharper. Note that no new peaks appear so no new structural units are formed.

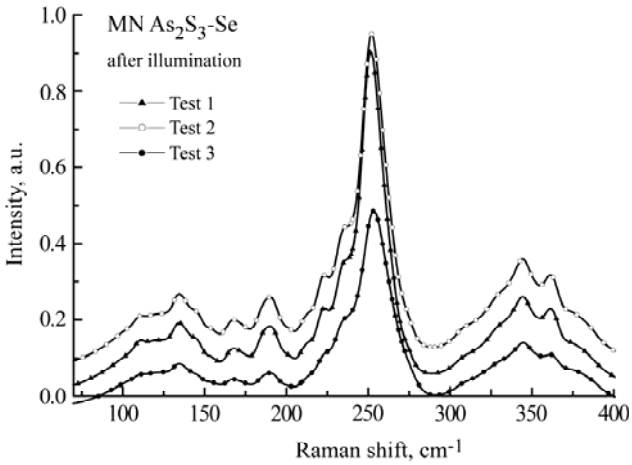

Fig. 6. Raman spectra of As_2S_3-Se MN with modulation period Λ = 50 nm (test 1), Λ = 25 nm (test 2), Λ = 15 nm (test 3) after illumination with wavelength 525 nm.

To demonstrate clearer the Raman spectra modifications under light, we plotted the subtraction of the Raman spectra before and after illumination (Figure 7). Each Raman spectrum was normalized by the area under the curve, and differential spectra

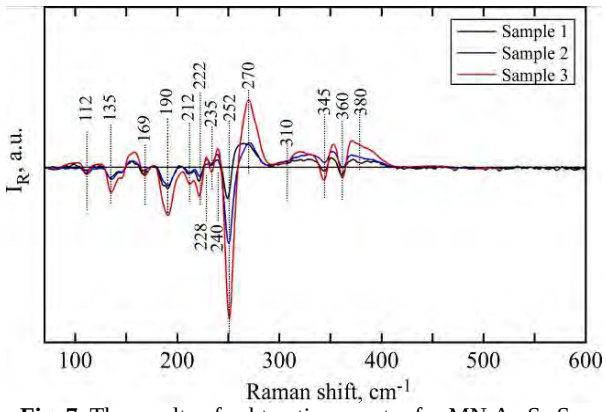

Fig. 7. The results of subtraction spectra for MN As_2S_3-Se.

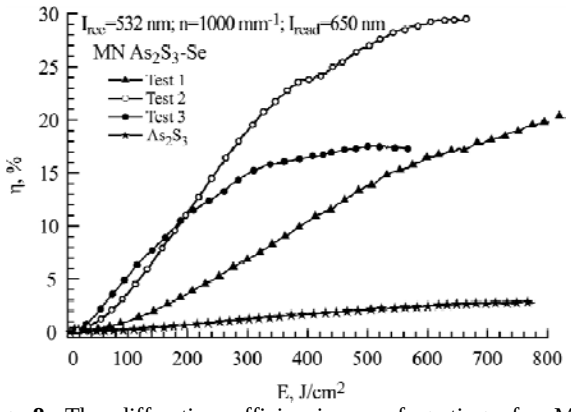

Fig. 8. The diffraction efficiencies η of gratings for MN As_2S_3-Se for different tests.

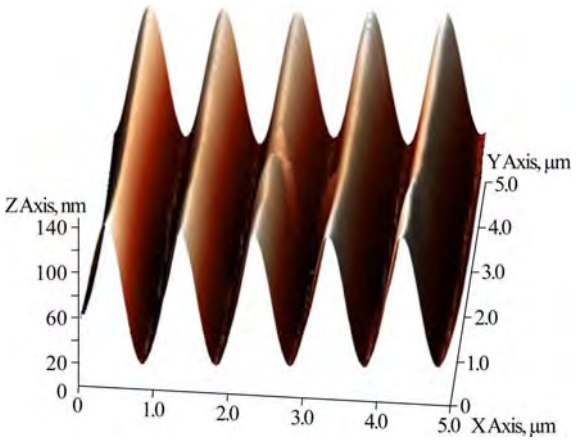

(a)

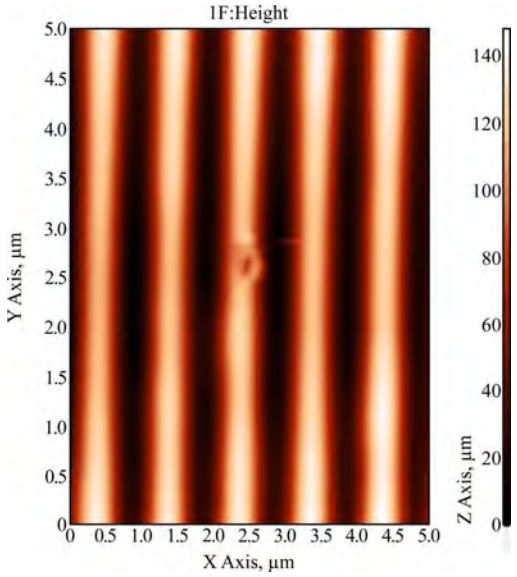

(b)

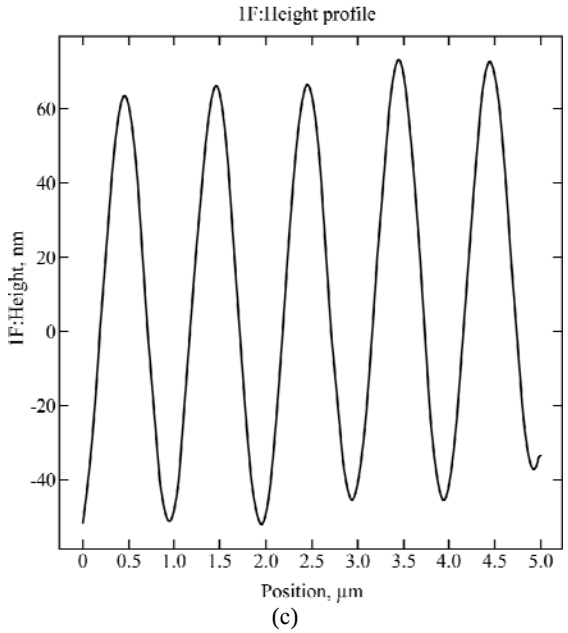

(c)

Fig. 9. Typical AFM view of recorded grating on As_2S_3-Se MN (test 2), (a) – 3-D view; (b) – 2-D view; (c) – surface profile.

for each NM were obtained by subtracting the appropriate spectra for the exposed and as-deposited sample (Figure 7). As can be seen from Raman subtracted spectra, the largest changes appeared in the spectra of sample 3 mainly due to the decrease of intensity of the Se main band at 252 cm^{-1}. Also in the exposed sample the bands get narrower in 120–240 cm^{-1} range and the band at 360 cm^{-1}, connected mainly with a "wrong" As-As bond in the As_4S_4 cages, and at the same time in the subtracted spectra a new band appeared at 228, 240 and 270 cm^{-1}, which is very close to a band for the $AsSe_3$

pyramidal units in the As_2Se_3 glass [14]. There is no measurable change discovered for a broad band at 495 cm^{-1} connected with the S-S bonds.

Changes in the Raman spectra for the exposed NMs allow us assuming that photostructural changes under exposition occur mainly due to a decrease in the amount of the Se rings, which means the inter-diffusion on the interface As_2S_3-Se of the NM and creation of new As-Se bonds. Decreasing the amount of "wrong" As-As bonds and appearing of new 228, 240 and 270 cm^{-1} bonds confirm this process and also could be connected with photo-polymerization of the As_2S_3 sublayers. From this point of view, the efficiency of photostructural changes in a NM should depend on the amount of the As_2S_3-Se interfaces, that is why the observed photoinduced changes are larger for a NM with a smaller periodicity. In addition, these photo-structural changes are favoured in chalcogenides because of a rapid localization of photo-excited carriers, a low energy of the valence alternation of pair defects and the freedom of low-coordination atoms to change their positions and bond configurations [17].

The diffraction efficiency changes were monitored in transmission mode during the recording time by the laser diode (LD) beam (λ_{read} = 650 nm). The diffraction efficiency η was measured in real-time at normal incidence of the LD beam by monitoring the intensity of the 1st order diffracted beam. Figure 8 shows the diffraction efficiency dependence on the exposure of a CW DPSS laser. It is seen that only for Test 3 the saturation of the diffraction efficiency value takes place. For other As_2S_3-Se MNs (Test 1, 2) and pure As_2S_3 we observed a constant rise of η but at a different rate. From the comparison of these dependences for different samples we can conclude that Test 2 has optimal recording properties meaning the maximum of both the value and the rate of the diffraction efficiency.

For pure Se we did not observe the gratings record because the recording wavelength λ_{rec} = 532 nm is absorbed in a thin (less than 10 nm) Se layer. Note the absorption coefficient of Se $\alpha > 10^5$ cm^{-1} for a wavelength of 525 nm, i.e. it is the region of high absorption for Se. The suppression of this irradiation takes place in a thin d < 10 nm selenium layer [9]. The active volume of the total MN structure is limited only in the near-surface layers. It is very important to underline that unlike many communications about the relief grating formation in the ChG films in our experiment no wet etching is needed for that.

The atomic-force microscopy (AFM) investi-gations of the recorded gratings allow the direct viewing of the relief surface. The surface of the holographic grating recorded on the As_2S_3-Se MN is shown in Figure 9a,b. It can be seen that the grating recording with the use of the As_2S_3-Se MN provides a high optical quality of the obtained relief with the depth of the grating surface about ~120 nm, at the total structure thickness of 2500 nm and the modulation period of layers 25 nm.

The grating profile is shown in Figure 9c. It can be seen that the depth of the grating surface is ~110 nm and the profile of the gratings obtained with the use of the As_2S_3-Se MN is close to the sinusoidal one.

CONCLUSION

The computer assisted cyclic thermal vacuum depositions of nanomultilayers process was tested. The technology allows depositing thin films with a nanometric monolayer thickness from 0.005 μm up to the total MN sample thickness of 3.0 μm. An alternate deposition of two materials from two separated boats on a continuously rotated glass substrate at room temperature in one vacuum deposition cycle was developed. Such approach for the samples layers configuration is aimed at investigating the size restriction of the constituent ChG layers of the samples. One deposition process gives a possibility to compare the Raman spectra of the constituent ChG layers and to study the influence of the constituent ChG layers thicknesses at the MN recording properties.

Three kinds of the MN As_2S_3-Se specimens have been prepared (see Table 1). These scaled samples have modulation periods covering one, two and three molecular and cluster dimensions for As_2S_3 and Se, which is characteristic to the so called medium-range order in glasses. This coincides with conclusions from paper [1].

We have established that the Raman spectra of the separated As_2S_3 and Se films are similar to those reported in literature [4–8]. For the as-deposited samples, the interfaces, which are the great fraction of the total volume of a sample, do not affect peak positions for both materials. It indicates that no new bonds are formed in comparison with the films prepared by conventional vacuum deposition methods. The changing of the peaks intensity, more pronounced in the Se film, is caused by a higher ordering of structure.

It was found that the photoinduced changes are larger for the NM with a shorter modulation period Λ = 15 nm (test 3), which is determined by the number of the As_2S_3-Se interfaces.

For the application perspective, the As_2S_3-Se MN with a modulation period of Λ = 25 nm is the most attractive, having the maximal diffraction efficiency (30%) at direct surface recording. A possible explanation of such behaviour of the MN may be the

presence of, at least, two processes influencing the recording. The first one is photo-diffusion taking place at the As_2S_3-Se interfaces, which is proved by the Raman spectra under illumination. The second one is the size restriction in the MN with the thickness of constituent layers around 2 medium range orders.

ACKNOWLEDGMENT

This work was supported by the grant "Development of Research Teams at the University of Pardubice" CZ.1.07/2.3.00/30.0058 from the Czech Ministry of Education, Youth and Sports.

REFERENCES

1. Tanaka K. Chalcogenide Glasses in: K.H.J. Buschow et al. (Editors-in-Chief), *Encyclopedia of Materials: Science and Technology*. Sec. Edition, Amsterdam: Elsevier, 2001, 1123–1131.
2. Saitoh A. and Tanaka K. *Appl Phys Lett.* 2003, **83**(9), 1725–1727.
3. Efimov O.M., Glebov L.B., Richardson K.A., Van Stryland E., et al. *Opt Mater*. 2001, **17**(3), 379–386.
4. Shimakawa K., Kolobov A., Elliott S.R. *Adv Phys*. 1995, **44**(6), 475–588.
5. Charnovych S., Kokenyesi S., Glodán Gy., Csik A. *Thin Solid Films*. 2011, **519**(13), 4309–4312.
6. Popescu M.A. *Non-Crystalline Chalcogenides*. Solid-State Science and Technology Library, Volume 8. Dordrecht: Kluwer Academic Publishers, 2000. 377 p.
7. Gouadec G. and Colomban P. *J Raman Spectrosc.* 2007, **38**(6), 598–603.
8. Lin Fang-Yin, Gulbiten Ozgur, Yang Zhiyong, et al. *J Phys D Appl Phys.* 2011, **44**, 045404.
9. Abashkin V., Achimova E., Kryskov Ts., et al. *Proc 2nd Int. Conf. of Nanotechnologies and Biomedical Engineering*. Chisinau, April 18–20, 2013, 254–257.
10. Holomb R., Mitsa V., Petrachenkov O., et al. *Phys Status Solidi C*. 2011, **8**(9), 2705–2708.
11. Röling C., Thiesen P., Meshalkin A., Achimova E., et al. *J Non-Cryst Solids*. 2013, **365**, 93–98.
12. Kovalsky A., Vlcek M., et al. *Proc. of SPIE, vol.7273, Conf. "Advances in Resist Materials and Processing Technology XXVI*. 72734A-1, 2009.
13. Kovalskiy A., Neilson J.R., Miller A.C., et al. *Thin Solid Films*. 2008, **516**(21), 7511–7518.
14. Naik Ramakanta, Ganesan R., Sangunni K.S. *J Non-Cryst Solids.* 2011, **357**, 2344–2348.
15. Nagels P. *Physics and Techniques of Semiconductors*. 1998, **32**(8), 958–963.
16. Tanaka K. *J Non-Cryst Solids*. 326&327, (2003), 21–28.
17. Sangunni K.S. *J of the Indian Institute of Science*. 2011, **91**(2), 295–302.

Received 03.08.15
Accepted 12.11.15

Реферат

Целью данного исследования является изучение структурных изменений в многослойной наноструктуре As_2S_3-Se и выяснение вклада слоев As_2S_3 и Se в наноструктурирование с помощью измерения спектров Рамана. Формирование наноструктуры As_2S_3-Se проводилось последовательным нанесением нанослоев As_2S_3 и Se. Зависимость дифракционной эффективности от дозы освещения CW DPSS лазером наблюдалась по пропусканию интенсивности 1^{ro} дифракционного максимума и измерялась в режиме реального времени и нормального падения луча лазерного диода (λ = 650 нм). Из сравнения полученных зависимостей для серии образцов была выбрана многослойная наноструктура с оптимальными характеристиками записи, то есть максимальная величина и скорость нарастания дифракционной эффективности. Данные результаты имеют практический интерес, так как позволяют существенно увеличить дифракционную эффективность рельефных решеток, сформированных прямой голографической записью.

Ключевые слова: халькогенидные стекла, наноструктуры, спектроскопия Рамана, поверхностная решетка.